Metal-Insulator Transition and Ferromagnetism in Diluted Magnetic Semiconductors

S.-R. Eric Yang[1,2] and A.H.MacDonald[2]
1)Department of Physics, Korea University, Seoul 136-701, Korea
2)Department of Physics, University of Texas at Austin, Austin TX 78712

We have investigated the interplay between the metal-insulator transition and ferromagnetism in $III_{1-x}Mn_xV$ semiconductors. Our study is based on a model in which $S = 5/2$ Mn local moments are exchange-coupled to valence band holes that interact via Coulomb interactions with each other, with ionized Mn acceptors, and with the antisite defects present in these materials. We find quasiparticle participation ratios consistent with a metal-insulator transition that occurs in the ferromagnetic state near $x \sim 0.01$. By evaluating the distribution of mean exchange fields at Mn moment sites, we provide evidence in favor of the applicability of impurity-band magnetic-polaron and hole-fluid models on insulating and metallic sides of the phase transition respectively.

PACS numbers: 75.50.Pp, 75.10.-b, 75.30.Hx

Introduction.- Recent progress [1] in the growth of diluted magnetic semiconductors semiconductors that exhibit ferromagnetism [2] at relatively high temperatures has suggested exciting new possibilities for devices that combine information processing and storage functionalities in a single material. It is generally accepted [3] that Mn acts as an acceptor in these semiconductors, that its half-filled d-shell contributes a $S = 5/2$ local moment [4–6] to the system's low-energy degrees of freedom, and that ferromagnetism is due to interactions between local moments that are mediated by valence-band holes. Recent experiments [7–10] demonstrate that ferromagnetism occurs in both metallic and insulating states, and that both magnetic and transport properties are sensitive to the Mn fraction x and to the density of compensating antisite and other defects in the material. The highest ferromagnetic critical temperatures (T_c) appear [10] to occur in the most metallic samples. The role of Coulomb interactions in the ferromagnetism in these materials is subtle. At high carrier densities, well on the metallic side of the metal-insulator transition, exchange and correlation in the hole system is expected [11] to enhance ferromagnetism. Well on the insulator side of the transition, however, Coulomb interactions create a Mott gap that increases the importance of randomness in Mn ion positions, suppresses carrier-hopping between Mn sides, and eventually turns off the coupling between local moments that can lead to ferromagnetism.

In this Letter we report on a numerical Hartree-Fock study of model (III,Mn)V ferromagnets in both metallic and insulating regimes. By evaluating the distribution of $T = 0$ Mn exchange mean-fields, defined precisely below, we find evidence that is generally supportive of the impurity-band magnetic-polaron [12–14] picture that has been used to describe ferromagnetism in the insulating regime, and of the hole-fluid picture that has been used [3,11,15,16] in the metallic regime. Our principle results are summarized in Figs. 1 and 2 where we plot *vs.*T the fraction of Mn sites that have exchange mean-fields larger than k_BT.

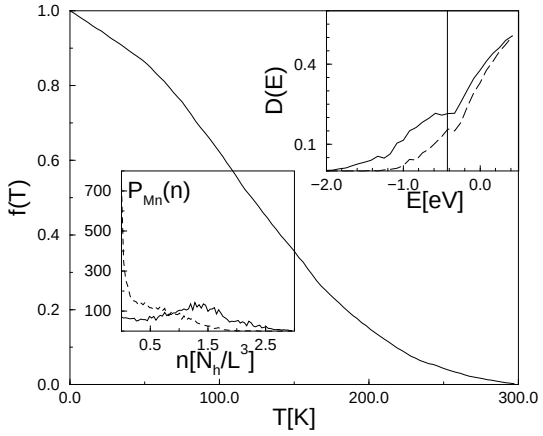

FIG. 1. $f(T)$, the fraction of Mn that experience a mean-field stronger than k_BT, *vs.* T in the metallic case. ($N_{Mn} = 1.0\text{nm}^{-3}$, $n_h = N_{Mn}/3$.) $P_{Mn}(n)$, the probability distribution function for partial hole densities at Mn sites in units of the average hole density, is plotted for majority (solid line) and minority (dashed line) spins in one inset and the quasiparticle density-of-states in the other inset. For this case the hole density at an isolated Mn is 1.63 times larger than the average hole density. The density of states $D(E)$ is per occupied hole with energies in eV. Note the anomaly at the Fermi energy E_F, indicated by a vertical line. The number of disorder realization is fifteen for $D(E)$ and ten for $f(T)$ and $P_{Mn}(n)$. A a simulation cell of side $L = 8$nm is used.

In the metallic case [17] ($x = 0.05$ and $p = 3.3 \times 10^{20}\text{cm}^{-3}$) the distribution of coupling strengths is peaked at a finite value close to its uniform hole-fluid value and all Mn ions are strongly coupled to holes. In the insulating case ($x = 0.01$ and hole density $p = 2.8 \times 10^{19}\text{cm}^{-3}$), on the other hand, we find that that vast majority of Mn spins are nearly free the few strongly

coupled Mn ions will form magnetic polarons that grow slowly in size and interact more strongly as the temperature is lowered. In the following sections we explain how these results were obtained and elaborate on their significance for models of diluted magnetic semiconductor ferromagnetism.

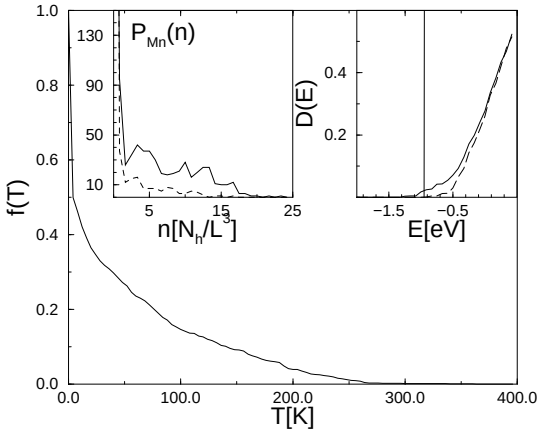

FIG. 2. As in Figure 1 but for the insulating case. ($N_{Mn} = 0.25\text{nm}^{-3}$ and $n_h = N_{Mn}/10$). The hole density at an isolated Mn site is 19.9 times larger than the average hole density in this case.

Model Hamiltonian.- Most theoretical work on (III,Mn)V ferromagnets has started from one of two idealized limits. Impurity-band models [12–14] achieve simplification by assuming that the holes that mediate interactions between Mn ion moments are strongly localized, whereas hole-fluid models achieve simplification by neglecting disorder due to Mn acceptors and other defects and treating it perturbatively in estimating transport coefficients. An insulator to metal phase transition occurs in these ferromagnets as Mn and hole densities increase; experimentally [1] it appears that the metal-insulator transition usually occurs near $x \sim 0.01$, likely depending on the density of compensating antisite defects, a quantity that is expected to be sensitive the details of sample-growth and annealing protocols. Although it is generally agreed that an impurity band picture should apply far on the insulator side of the transition and a hole-fluid model far on the metallic side of the transition, it has not been clear which approach is a better starting point in the experimentally relevant parameter ranges. We address this issue by examining the ferromagnetic ground state using a model, and an approximation scheme, that captures the physics of both limits correctly. Our study is built on $\vec{k} \cdot \vec{p}$ envelope-function approach description of the valence band [18] and a Hartree-Fock description of interactions.

The four terms in the single-particle part of our band electron model Hamiltonian, $H^0 = H^K + H^{K.ex.} + H^{Mn-h} + H^{as-h}$, require some discussion. $H^{K.ex.}$ represents the kinetic exchange interaction between Mn local moments, assumed to be aligned in the ferromagnetic system ground state [19], H^{Mn-h} represents the attractive Coulomb interaction between an ionized Mn^{2+} acceptor and a valence band hole. In an envelope function formalism, central cell corrections to this interaction are necessary [20] to achieve an accurate description of the isolated bound-acceptor limit. H^{as-h} describes the repulsive interaction between holes and antisite defects (represented as sites with charge +2). These defects act as deep donors partially compensating the Mn acceptors and reducing the overall hole density, and provide an important additional scattering center. H^K is the usual kinetic energy term. In this study we ignore [8,16,21] mixing between heavy and light hole bands by using a simple parabolic band approximation.

$$H^0 = \frac{-\hbar^2}{2m}\vec{\nabla} + \frac{1}{2}S\sum_I \hat{\Omega}_I \cdot \vec{\tau} J(\vec{r} - \vec{R}_I) + \sum_I \left(-\frac{e^2}{\epsilon|\vec{r} - \vec{R}_I|} - V_0 e^{-|\vec{r}-\vec{R}_I|^2/r_0^2}\right) + \sum_K \frac{2e^2}{\epsilon|\vec{r} - \vec{R}_K|}. \quad (1)$$

Here $J(\vec{r}) = (J_{pd}/(2\pi a_0^2)^{3/2}) \exp(-r^2/2{a_0}^2)$, $\vec{\tau} = (\tau_x, \tau_y, \tau_z)$ is the Pauli spin matrix vector, I labels Mn sites, K labels antisite defect sites, and $\hat{\Omega}_I$ is the orientation of the I^{th} Mn spin. The term in the potential proportional to V_0 is the central cell correction. Both Mn ions and antisites were distributed randomly [22] in a cube of side L. The long range of the Coulomb interaction requires overall charge neutrality so that $n_h - N_{Mn} + 2N_{as} = 0$, where n_h is the density of holes, N_{Mn} the density of Mn ions and N_{as} the density of antisites. In the ground state, all Mn spins are oriented along the $\hat{z}$ direction and H^0 is block diagonal in its spin indices. In the spin wave configurations discussed below, $\hat{x}$ and $\hat{y}$ components of the spins are present, doubling the dimension of the matrix that must be diagonalized numerically. The wavevector cutoff in the quasiparticle wavefunction expansion [23] was tested by computing the binding energy of a hole to an isolated Mn, comparing with the results of Bhattacharjee and Benoit a la Guillaume [20] who find that a binding energy of 112meV, 86 meV when the kinetic exchange term is neglected, and 68meV when the central cell correction is also neglected. Our results are 124meV, 88 meV, and 48meV respectively, demonstrating an adequate description of the completely isolated Mn limit.

In order to capture the correct physics of both metallic and impurity band limits, hole-hole interactions must be described using an approximation that accounts for screening effects in the metallic regime and avoids artificial self-interaction effects in the localized regime, motivating our use of Hartree-Fock (HF) theory [24]. The HF quasiparticle Hamiltonian is $H^{HF} = H^0 + (V^H + V^X)$

where the Hartree and Fock matrix elements, $V^H_{\vec{k}\sigma,\vec{k}'\sigma'}$ and $V^X_{\vec{k}\sigma,\vec{k}'\sigma}$, can be expressed in terms of the density matrix. We evaluate the density matrix in the k-space representation used to expand our envelope function quasiparticle wavefunctions: $\rho_{\vec{k}\sigma,\vec{k}'\sigma'} = \sum_\alpha n_\alpha c^{(\alpha)}_{\vec{k}\sigma} c^{(\alpha)*}_{\vec{k}'\sigma'}$, where $|\alpha\rangle = \sum_{\vec{k}\sigma} c^{(\alpha)}_{\vec{k}\sigma}|\vec{k}\sigma\rangle$, and n_α is a quasiparticle occupation number. Our HF scheme becomes *exact* in the strongly localized limit, since a localized quasiparticle does not interact with itself, but is expected to overestimate inhomogeneity in the metallic limit because it neglects quantum fluctuations in the many-hole state.

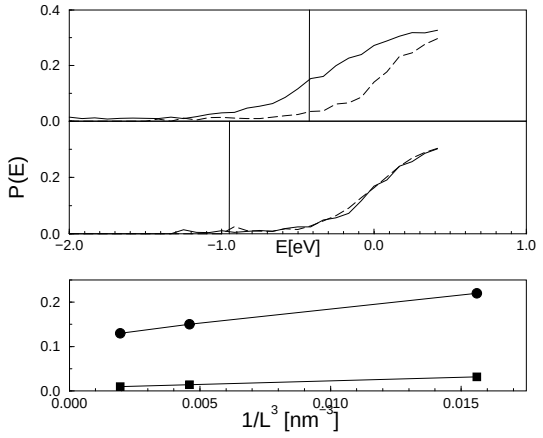

FIG. 3. Participation ratios *vs.* energy in a simulation cell of side $L = 8$nm for majority (solid line) and minority (dashed line) quasiparticles. The Fermi energies are indicated by solid vertical lines. The upper panel is for the metallic case of Fig. 2 and the middle panel is for the insulating case of Fig. 3 and these results were obtained by averaging over 15 disorder realizations. The bottom panel shows the system size dependence of majority-spin participation ratios at the Fermi energy for the two cases.

Participation ratios.- In order to verify that our model correctly describes the metal-insulator transition in these materials, we measured the localization properties of our Hartree-Fock quasiparticles by evaluating their participation ratios, $P_\alpha = 1/(L^3 \int d^3r |\Psi_\alpha(\vec{r})|^4)$, where $\Psi_\alpha(\vec{r}) = \langle\vec{r}|\alpha\rangle$ is a normalized quasiparticle wavefunction. (For a localized state $P_\alpha \sim (\xi_\alpha/L)^3$, where ξ_α is the localization length.) Fig. 3 compares participation ratios evaluated at $x = 0.05$ and 0.0125, assuming compensated carrier densities $n_h = N_{Mn}/3$ and $n_h = N_{Mn}/10$, respectively. The participation fractions extrapolated to infinite volume are clearly finite and therefore consistent with metallic transport at $x = 0.05$ whereas they are consistent with zero and localized quasiparticles at $x = 0.0125$, in agreement with experiment.

Impurity-Band Picture vs.Hole-Fluid Picture.- The exchange mean-fields used to construct Fig. 1 and Fig. 2 are given by $H_{eff,I} = \int d\vec{r} J(\vec{r} - \vec{R}_I)(n_\downarrow(\vec{r}) - n_\uparrow(\vec{r}))/2 \approx J_{pd}(n_\downarrow(\vec{R}_I) - n_\uparrow(\vec{R}_I))/2$ where the partial densities are determined by solving the Hartree-Fock equations self-consistently. In the extreme impurity band limit, $H_{eff,I}$ would have the value $J_{pd}n_{max}/2 \approx 25$meV for a fraction n_h/N_{Mn} of the local moments and much smaller values for all others. Our findings are in qualitative agreement, although the peak H_{eff} value is somewhat smaller and there is no sharp peak in the distribution function near the peak value, presumably because of the variable Mn and antisite defect environment experienced by localized holes. (The shallow impurity Bohr radius a^*_B calculated using the heavy-hole mass is $\sim$ 1.0nm; the peak hole density, 4.9×10^{20}cm^{-3} is slightly larger than the shallow impurity value because of central cell corrections.) Kaminski and Das Sarma [13] have recently estimated the impurity-band magnetic polaron model T_c, relating it to N_{Mn}, n_h and the maximum mean-field exchange coupling by $T_c \sim 0.5(N_{Mn}/n_h)^{1/2}({n_h a^*_B}^3)^{1/6} H_{max} \exp(-0.86/{n_h}^{1/3}a^*_B)/k_B$. Naively applying this formula to our $x = 0.01$ case with the shallow impurity Bohr radius yields $T_c \sim 15K$. Note that T_c is expected to decrease rapidly at lower hole densities because of the weakening magnetic polaron coupling. These estimated T_c's are somewhat larger than what has typically been observed at $x \sim 0.01$ in (Ga,Mn)As, possibly because the theory neglects Pauli exclusion principle effects, superexchange interactions, that favor opposite orientations of nearby impurity-band holes and oppose ferromagnetism. Nevertheless, it appears that this picture provides an excellent qualitative description of ferromagnetism at $x \sim 0.01$ and smaller.

In the metallic case, the exchange mean-field distribution differs qualitatively, with strong couplings common and few weakly coupled moments. Our results likely overestimate the degree of density variation in samples with $x \sim 0.05$, both because we have neglected Mn acceptor-antisite correlations [22] and because of our use of the Hartree- Fock approximation. (The corresponding self-consistent Hartree calculations lead to more sharply peaked Mn site majority-spin density distributions.) We note that the most likely hole density at a Mn site is approximately 1.5 times larger than the average hole density and that the most likely mean-field coupling strengths are again somewhat larger than the uniform hole-fluid value $H_{fl} = nJ_{pd}/2 \approx 190$K.

There are important differences between metallic and insulating cases in the physics that controls T_c. The metallic T_c can be limited either [28,25] by the system's stiffness against collective magnetization orientation variation, or if the stiffness is large enough by the competition between local moment entropy, exchange interactions, and the band energy cost of hole-spin polarization that is captured by the hole-fluid mean-field-theory T_c expression [26]. We have estimated the magnetic stiffness of both insulating and metallic states by evaluating the HF electronic energy cost of an imposed spin-wave with wavevector Q. If disorder were neglected, the pro-

cedure we follow in evaluating spin spin-wave energies differs from the theory [27] of König *et al.* only through retardation effects.

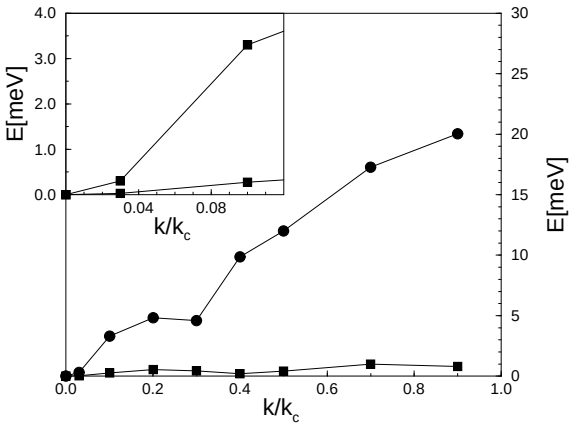

FIG. 4. Average spin-flip energy *vs.* wavevector. The upper curve is for the metallic case of Fig.1 while the lower curve is for the insulating case of Fig.2. The wavevector is normalized to a Debye wavevector defined by the Mn density in each case, $k_c = (6\pi^2 N_{Mn})^{1/3}$. The inset shows a magnified view of the small wavevector regime.

Figure 4 displays average spin reversal energies for metallic and insulating states. Note that the energy cost of slow (long wavelength) spin-direction variations is extremely small in the insulating case because these are sensitive mainly to the weak interactions between magnetic polarons that are necessary for long-range magnetic order. It follows that mean-field will completely fail in estimating the critical temperature of insulating DMS ferromagnets. The energy cost for spin-direction variations that we find in the metallic case is in qualitative agreement with hole-fluid model results, although it is larger at short wavelengths. In the hole-fluid mean-field theory the energy cost of spin-direction variations would equal H_{fl} at all wavevectors. It follows that for the parabolic band model we have studied substantial corrections [28,25] would apply to its mean-field T_c. It is important to note, however, that valence band spin-orbit interactions stiffen collective spin-variations in these ferromagnets [29], reducing corrections to mean-field-theory T_c estimates.

SREY is supported in part by the KOSEF Quantum-functional Semiconductor Research Center at Dongkuk University. Work at the University of Texas was supported by by the Welch foundation and by DARPA/ONR Award No. N00014-00-1-095.

[1] H. Ohno, J. Magn. Magn. Mater. **200**, 110 (1999) and work cited therein; M.L. Reed *et al.*, Appl. Phys. Lett. **79**, 3473 (2001); Y.D. Part *et al.*, Science **295**, 651 (2002); T. Slupinski *et al.*, Appl Phys. Lett. (to appear) (2002); X. Chen *et al.*, preprint (2001); N. Theodoropoulou *et al.*, eprint [http://arXiv.org/abs/cond-mat/0201492].

[2] H. Munekata *et al.*, Phys. Rev. Lett. **63**, 1849 (1989); H. Ohno *et al.* Phys. Rev. Lett. **68**, 2664 (1992).

[3] J. König *et al.*, eprint [http://arXiv.org/abs/cond-mat/0111314] and work cited therein.

[4] J. Szczytko *et al.*, Phys. Rev. B, **60**, 8304 (1999).

[5] M. Linnarsson *et al.*, Phys. Rev. B, **55**, 6938 (1997).

[6] O.M.Fedorych *et al.*, eprint [http://arXiv.org/abs/cond-mat/0106227].

[7] H. Ohno, Science **281**, 951 (1998).

[8] F. Matsukura *et al.*, Phys. Rev. B, **57**, R2037 (1998).

[9] T. Hayashi *et al.*, Appl. Phys. Lett. **78**, 1691 (2001).

[10] S.J. Potashnik *et al.*, Appl. Phys. Lett. **79** 1495 (2001) and submitted to Phys. Rev. Lett.

[11] T. Jungwirth *et al.*, Phys. Rev. B **59**, 9813 (1999); T. Jungwirth *et al.*, eprint [http://arXiv.org/abs/cond-mat/0201157].

[12] M. Berciu and R.N. Bhatt, Phys. Rev. Lett. **87**, 7203 (2000); Adam C. Durst, R.N. Bhatt, and P.A. Wolff, eprint [http://arXiv.org/abs/cond-mat/0111497].

[13] A. Kaminski and S. Das Sarma, eprint [http://arXiv.org/abs/cond-mat/0201229].

[14] C. Timm, F. Schäfer, and F. von Oppen, eprint [http://arXiv.org/abs/cond-mat/0111504].

[15] T. Dietl *et al.*, Science **287**, 1019 (2000); T. Dietl *et al.*, Phys. Rev. B **63**, 195205 (2001).

[16] M. Abolfath *et al.*, Phys. Rev. B 63, 054418 (2001).

[17] The carrier density in annealed samples at $x = 0.05$ has been extracted from high-field Hall effect data by T. Omiya *et al.*, Physica E **7**, 976 (2000). The degree of compensation at $x = 0.01$ is less accurately known and likely to be sample dependent.

[18] Density-functional electronic-structure techniques have been applied to these materials and will be important in refining models of the type we study. This approach has not yet advanced sufficiently to address the questions of interest here, partly because the local density approximation overestimates exchange coupling strengths. For a review see S. Sanvito, G. Theurich and N.A. Hill, eprint [http://arXiv.org/abs/cond-mat/0111300].

[19] J. Schliemann and A.H. MacDonald, eprint [http://arXiv.org/abs /cond-mat/0107573] have suggested that non-collinear ground state Mn ion orientations can occur in models with kinetic exchange only. Our calculations demonstrate that Coulomb interactions favor collinear configurations, although non-collinear configurations are still likely in the insulating regime. Quantum fluctuations in Mn ion orientations are weak because of the large separation between the energy scales for band electron and Mn ion spin fluctuations.

[20] A.K. Bhattacharjee and C. Benoit à la Guillaume, Solid State Comm. **113**, 17 (2000).

[21] Gergely Zarand and Boldizsar Janko, eprint [http://arXiv.org/abs/cond-mat/0108477].

[22] C. Timm *et al.* have pointed out that defect correlations,

which we do not include here, will reduce the importance of disorder, expanding the validity range of the hole-fluid picture.

[23] The model Hamiltonian parameters we use are those generally accepted for (Ga,Mn)As, the best understood (III,Mn)V ferromagnet. $J_{pd} = 0.1$eV nm^3, $a_0 = 0.3$ nm, $\epsilon = 10$, $V_0 = 2.5eV$ and $r_0 = 0.259$ nm. We diagonalize the HF Hamiltonian in a plane wave representation, using periodic boundary conditions in the simulation cell. For different system sizes we maintain the cutoff wavevector $k_{max} = \pi$ nm^{-1}.

[24] S.-R. Eric Yang and A. H. MacDonald, Phys. Rev. Lett. **70**, 4110 (1993); S.-R. Eric Yang, A. H. MacDonald, and B. Huckestein, Phys. Rev. Lett. **74**, 3229 (1995); S.-R. Eric Yang, Ziqiang Wang, and A. H. MacDonald, Phys. Rev. B **65**, 041302 (2001).

[25] A. Chattopadhyay, S. Das Sarma and A.J. Millis, Phys. Rev. Lett. **87** 227202 (2001).

[26] T. Dietl *et al.*, Phys. Rev. B **55**, R3347 (1997).

[27] J. König, H.H. Lin, A.H. MacDoanld, Phys. Rev. Lett **84** 5628 (2000).

[28] J. Schliemann *et al.*, Appl. Phys. Lett. **78**. 1550 (2001); J. Schliemann, J. König and A.H. MacDonald, Phys. Rev. B **64**, 165201 (2001).

[29] J. König, T. Jungwirth, and A.H.MacDoald, Phys. Rev. B, **64**, 184423 (2001).